

Elongational Flow Studies on the Phase Separation of Hydroxypropylcellulose Solution

Syuji Fujii, Naoki Sasaki, Mitsuo Nakata

Division of Biological Sciences, Graduate School of Science, Hokkaido University, Kita-ku, Sapporo 060-0810, Japan

Received 8 August 2001; accepted 11 April 2002

ABSTRACT: The phase separation of hydroxypropylcellulose (HPC) in a mixed solvent of glycerol and water was investigated by an elongational flow birefringence method. In the one-phase region, the elongational flow birefringence had the characteristics of a typical coil-stretch transition-like pattern with a critical elongational strain rate $\dot{\epsilon}_c$. $\dot{\epsilon}_c$ increased monotonously with temperature, but in the vicinity of the phase-separation point, $\dot{\epsilon}_c$ began to decrease even in the one-phase region. In the two-phase region, the flow-induced

birefringence pattern contained both a rigid rod-like response and the coil-stretch transition-like response of a flexible polymer. The appearance of the rod-like birefringence pattern indicates the association of HPC chains to form a precursor of the liquid-crystalline phase formation. © 2002 Wiley Periodicals, Inc. *J Appl Polym Sci* 86: 2984–2991, 2002

Key words: phase separation; rheology; water-soluble polymers

INTRODUCTION

It is well known that the hydroxypropylcellulose (HPC) aqueous solution exhibits a lower critical solution temperature (LCST).^{1–4} Figure 1 shows the schematic diagram of the HPC–water system obtained so far. The chimney-like two-phase region runs through the one-phase region. The phase diagram with the chimney-like two-phase region has been investigated to be characteristic for semirigid molecules such as poly(γ -benzyl-L-glutamate) (PBLG), including HPC.^{5–8} A one-phase but more concentrated solution than the chimney-like two-phase region exhibits a transition from an optically anisotropic one-phase solution to a two-phase solution with an increase in temperature. In the case of HPC, this optical anisotropy in the one-phase region has been suggested to be due to the appearance of a liquid-crystalline phase (cholesteric order).^{1–8} On the other hand, even in lower concentrations than the chimney-like two phase region, it has also been reported that the HPC aqueous solution exhibits a transition from an isotropic one-phase solution to an anisotropic two-phase solution (liquid-crystalline phase) with an increase in temperature.^{2–5} Although both the phase diagram and the liquid-crystalline formation indicate the rigid rod-like nature of HPC, the persistence length of HPC was reported to be about 70 Å, which is far from rigid and rod-like.^{5,6} Many investigators have suggested that the phase sep-

aration and evolution of the HPC system are significantly affected by the liquid-crystalline phase formation, although the molecular mechanism of the liquid-crystalline formation is still unknown.

Our aim in this work was to elucidate the molecular origin of the liquid-crystalline formation process of the HPC solution by investigating rheologically its phase-separation dynamics. For this, we employed an elongational flow birefringence method because this method is known to be very sensitive to molecular conformational change as compared with traditional shear rheometry. On the basis of the elongational flow field-induced birefringence below and above the phase-separation temperature, we discuss here the development of the conformation of HPC during the liquid-crystalline phase formation accompanied by phase separation.

Elongational flow birefringence

The response of polymer molecules to an elongational flow field is intrinsically different from the response to a shear flow field. In a shear flow, the extensional and rotational components of the strain rate are equal, and an extended state and/or alignment of molecules is not achieved. In an elongational flow field, there is no rotational component at all. When the hydrodynamic frictional force by an elongational field exceeds the entropic force of a polymer chain, the polymer chain is expected to be in a runaway process for an extended conformation. The elongational strain rate ($\dot{\epsilon}$) for the onset of the runaway process is referred to as the critical elongational strain rate ($\dot{\epsilon}_c$). This expectation was rationalized as the coil-stretch transition by de

Correspondence to: N. Sasaki (sasaki@gogh.sci.hokudai.ac.jp).

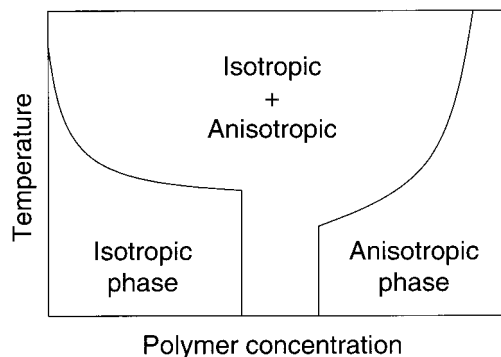


Figure 1 Schematic phase diagram for HPC solutions.

Genes⁹ and was confirmed empirically by Keller and Odell.¹⁰

When applying an $\dot{\epsilon}$ that exceeds $\dot{\epsilon}_c$, the flexible polymer solution shows a flow-induced birefringence (Δn) along the pure elongational flow field. Then, the birefringence increases rapidly with $\dot{\epsilon}$. This phenomenon is a manifestation of the coil-stretch transition. On the other hand, rod-like molecules become aligned along the flow direction with an increase in $\dot{\epsilon}$. Their birefringence pattern differs significantly from that of a flexible chain at the point that there is no criticality in the appearance of Δn , and the birefringence does not localize along the pure elongational field.^{10–13} If a polymer chain undergoes a conformational transition from a rod-like structure to a flexible coil and vice versa, the transition process will be well documented by the observation of an elongational Δn . On the basis of this concept, a conformational change of macromolecules, such as the collapsing of a secondary structure of DNA and collagen or a morphological variation in a single polymer chain, has been investigated.^{11–14}

EXPERIMENTAL

Materials

The HPC sample used in this study was purchased from Scientific Polymer Production Inc. (Ontario, NY). The weight-average molecular weight (M_w) of HPC in methanol was confirmed by a static light-scattering (SLS) method. The refractive index increment (dn/dc) of HPC in methanol at temperature (T) = 50°C was measured with a Brice-type differential refractometer (Narumi NLM-II, Tokyo) with a halogen lamp ($\lambda_0 = 436 \text{ \AA}$) source. The value of dn/dc was 0.1575 at $T = 50^\circ\text{C}$. This value was used for SLS experiments to determine the actual M_w of HPC. The results of an SLS experiment were analyzed by a Zimm plot. The value of M_w obtained from the Zimm plot was $M_w \approx 437,000$. For the flow experiments, we used glycerol and distilled water as a mixed solvent. The addition of glycerol to water was performed to make the solvent viscous. Because an increase in the solvent viscosity

(η_s) slows down the relaxation of a polymer, it is possible to measure the flow birefringence, even if the polymer concentration is in the dilute region. Glycerol, which was supplied by Wako Pure Chemical Industries, Ltd. (Osaka, Japan), was used without further purification. The distilled water was prepared and deionized by Milli-RO, Milli-Q (Millipore, Inc., Bedford, MA). A mixed solvent of glycerol and distilled water that was prepared with a weight fraction of glycerol of 33.6 wt % was used in all experiments.

Before the commercial HPC sample was used, it was purified by dissolution in distilled water. The solutions were stirred for more than 1 day, and they were then filtered to eliminate some insoluble particles and freeze dried. The desired amounts of HPC were dispersed in the mixed solvent and dissolved thoroughly by stirring for at least 1 week.

Methods

Cloud point temperature (T_p)

We determined T_p directly by observing the turbidity and by measuring transmitted light intensity (I_0). The appearance of turbidity was visually observed according to the method of Chevillard and colleagues.^{15,16} After the observations, the temperature of the thermally controlled bath was increased, and this procedure was repeated. I_0 of the sample solution was measured at temperatures from 20 to 40°C with a He-Ne laser as an incident beam. The optical path length of the sample cell was 1 cm. I_0 at each temperature was detected with a photodiode. The observed turbidity corresponded to the attenuation of I_0 . In the one-phase region, I_0 did not change with temperature; I_0 as a function of temperature manifested as a plateau. In the vicinity of the phase-separation temperature, I_0 decreased with an increase in temperature, reflecting the association of polymer molecules that originated from the phase-separation phenomenon. T_p was determined as the temperature at the intersecting point of the tangential line for the I_0 -temperature curve at the one-phase region and that the decreasing region in I_0 -temperature curve near the phase-separation temperature. The apparent spinodal temperature (T_s) was determined as the temperature at which the I_0 was extrapolated to zero, following the method of Tanaka et al.¹⁷ The phase diagram was investigated over the polymer concentration range of $1 \leq c \leq 100 \text{ g/L}$. In this concentration range, all HPC solutions were isotropic in the one-phase region.

Elongational flow

An elongational flow field was generated by a four-roll mill apparatus, which was originally used by Taylor for the investigation of a liquid droplet in the flow

field.¹⁸ Details about the four-roll mill set-up can be found elsewhere.¹¹ The extensional strain rate of the four-roll mill apparatus was determined geometrically, according to Torza.¹⁹ Our four-roll mill apparatus could generate a flow field with strain rate up to 160 s^{-1} . All measurements of elongational Δn were performed 30 min after the temperature had been changed to ensure thermal equilibrium of the sample solution and to exclude the effect of time evolution of the cluster formation.

RESULTS AND DISCUSSION

Phase diagram

It is well known that HPC shows LCST-type phase behavior. Figure 2 shows a phase diagram of HPC in the mixed solvent of glycerol and water observed in this study. In our system, due to the addition of glycerol, T_p was lower by about 10°C than that in the HPC-water system in the literature.¹⁻³ Sarkar suggested that the addition of glycerol enhances the dehydration of the HPC system and alters the intermolecular hydrogen bonding system.²⁰ Our phase diagram had a local maximum point near 60 g/L , which is denoted by $T_{p,\text{max}}$. In this experiment, $T_{p,\text{max}}$ was about 25.3°C . In higher concentrations than those showing $T_{p,\text{max}}$, T_p was gradually reduced with the concentration. This reduction seemed to form the upper part of the chimney-like-shaped narrow biphasic region.¹⁻³

Guido observed the appearance of cholesteric droplets in a two-phase region by microscopy.¹ In this experiment, the appearance of the liquid-crystalline droplet was confirmed by observation of the birefringence with the four-roll mill apparatus between crossed polars in the absence of flow near the T_s .

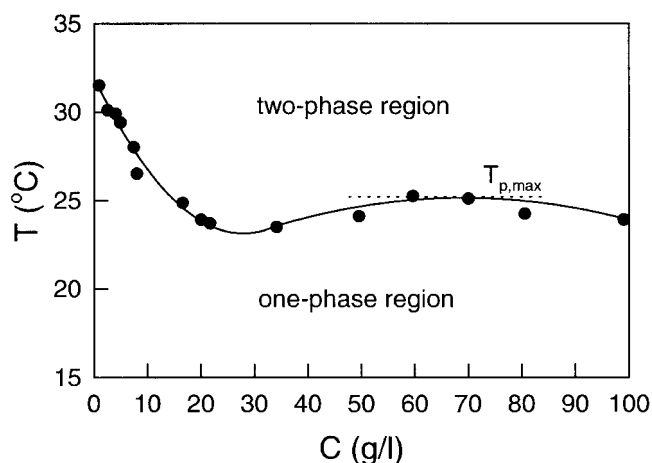


Figure 2 Phase diagram of HPC in a mixed solvent of glycerol and water at a weight fraction of glycerol of 33.6 wt % in water. Filled circles coincide with T_p .

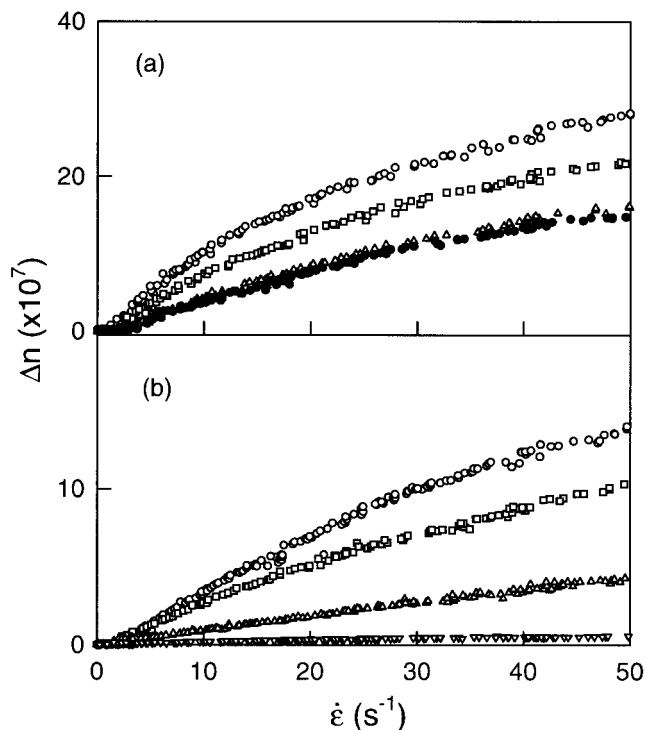


Figure 3 Elongational Δn as a function of $\dot{\epsilon}$ for the HPC concentration of 19.99 g/L . Δn as a function of $\dot{\epsilon}$ was measured at various temperatures. (a) Before the phase separation and (b) after the phase separation, all the Δn versus $\dot{\epsilon}$ curves, except for the temperature of 32.3°C , had $\dot{\epsilon}_c$ s indicating a coil-stretch transition. Symbols in (a) correspond to 5.3 , 10.8 , 19.7 , and 23.8°C , respectively, mentioned previously, and symbols in (b) are 25.9 , 28.5 , 31.3 , and 32.3°C , respectively, mentioned previously.

Properties in elongational flow

Elongational flow birefringence in HPC

Figure 3(a,b) shows the typical elongational Δn as a function of $\dot{\epsilon}$ in the one-phase and two-phase regions, respectively. In both figures, the HPC concentration is $c = 19.99 \text{ g/L}$. In the one-phase region, in the lower $\dot{\epsilon}$ region, there was a $\dot{\epsilon}_c$ for the Δn that was localized at the pure elongational flow field. These are the typical features of a coil-stretch transition-like conformational change. $\dot{\epsilon}_c$ is related to the longest relaxation time (τ) of the polymer chain by the relation

$$\dot{\epsilon}_c \tau \sim 1 \quad (1)$$

In the one-phase region, the decrease in birefringence intensity with temperature suggests a tendency of HPC chain segments to have had a random orientation due to the Brownian motion and the increase in the entropic restoring force of the HPC chains. The entropic restoring force depends on temperature, solvent quality, and chain properties, such as flexibility and end-to-end distance. The temperature dependence of birefringence intensity could have been re-

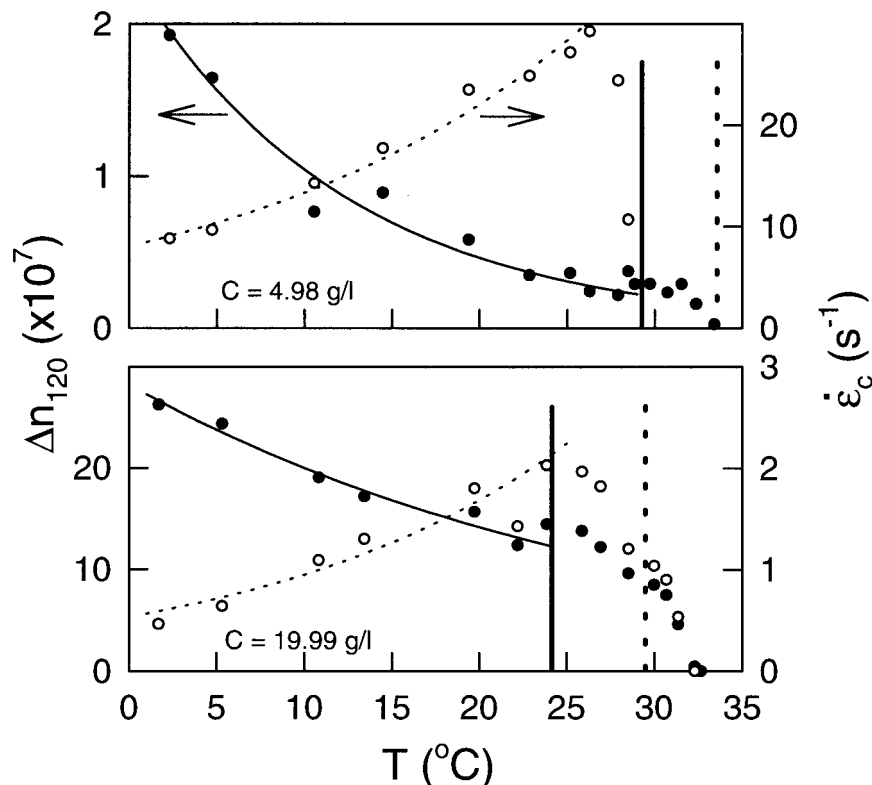


Figure 4 Temperature dependence of (○) $\dot{\epsilon}_c$ and (●) Δn_{120} at $\dot{\epsilon} = 120 \text{ s}^{-1}$ for HPC solutions of 4.98 and 19.99 g/L. The vertical solid line indicates T_p .

lated to the relaxation time of HPC solution because the relaxation time includes temperature-dependent terms such as Flory radius and η_s . The coil-stretch transition-like pattern in the two-phase region near T_p suggests that the polymer chain or polymer chain cluster underwent deformation until the liquid-crystalline phase formation occurred above the T_s . Figure 4 shows the temperature dependence of $\dot{\epsilon}_c$ and the birefringence intensity at $\dot{\epsilon} = 120 \text{ s}^{-1}$ (Δn_{120}) at indicated HPC concentrations. The vertical solid and dotted lines indicate T_p and T_s , respectively. The solid and dotted curves are described by the single exponential curve; that is, the Arrhenius law holds. T_{peak} and T_{van} are defined as the peak in the $\dot{\epsilon}_c(T)$ versus T plot and the vanishing point of Δn_{120} , respectively. In HPC solutions of 4.98 g/L, $\dot{\epsilon}_c$ deviated from the exponential curve at T_{peak} , which was lower than T_p , and reduced to the vanishing point of birefringence intensity [$\Delta n_{120}(T_{\text{van}}) = 0$]. Because T_{van} almost agreed with the T_s , it is possible to describe $T_{\text{van}} \approx T_s$, where the liquid-crystalline droplet seemed to be not deformed by the elongational flow field. Δn_{120} decreased with temperature below T_p ; then, Δn_{120} manifested a different temperature dependence at T_{peak} . This change in the temperature dependence of Δn_{120} and $\dot{\epsilon}_c$ indicated a change in the response of molecules to the elongational flow field, that is, a change in the chain flexibility at T_{peak} . This temperature dependence of Δn_{120} and

$\dot{\epsilon}_c$ was observed at lower concentration regions up to 8 g/L. On the other hand, at higher concentrations, for example, at 19.99 g/L, T_{peak} almost agreed with T_p . In the two-phase region, T_{van} was slightly different from T_s . The concentration dependence of the response of polymer molecules to an elongational flow field was probably due to the interaction through entanglements among polymer chains. Further investigation of the concentration dependence of the response of polymers to the elongational flow is needed.

Molecular size (R) evolution with temperature

To make clear the molecular process occurring in the vicinity of T_{peak} , we investigated the change in the molecular association size. Figure 5(a) shows Δn_{120} and $\dot{\epsilon}_c$ presented in Figure 4 plotted against η_s .²¹ We made the η_s axis scale by rescaling the temperature axis in Figure 4, where small and large η_s 's correspond to higher and lower temperatures, respectively. An increase in temperature, that is, a decrease in η_s , caused a decrease in the friction between polymer and solvent molecules. Therefore, a decrease in the birefringence intensity Δn_{120} with decrease in η_s in the one-phase region corresponded to a decrease in extensional force exerted on HPC chains. The sudden drop in Δn_{120} with a decrease in η_s was attributed to an increase in the turbidity originating from the associa-

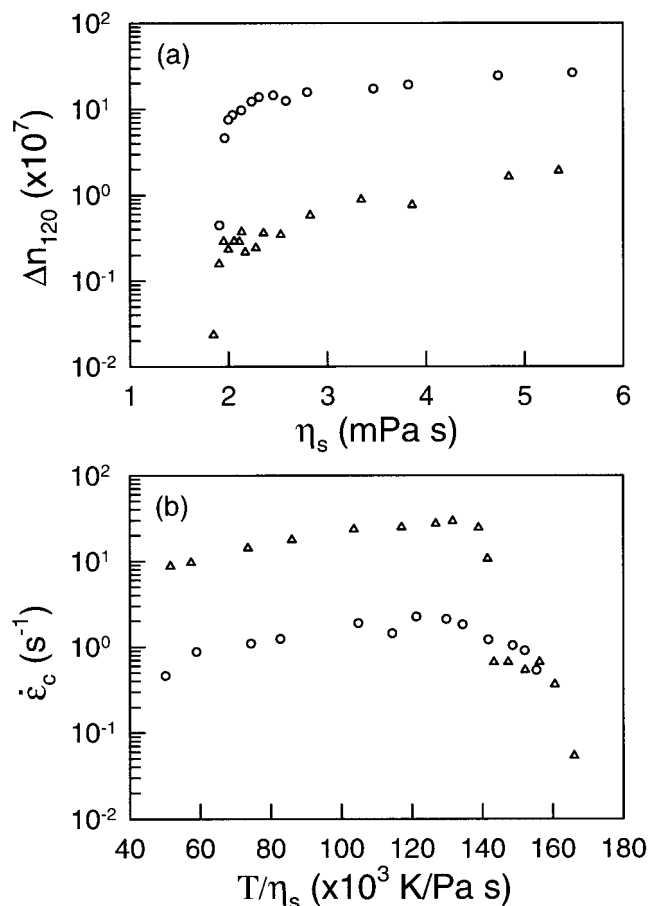


Figure 5 (a) Δn_{120} as a function of η_s . (b) $\dot{\epsilon}_c$ as a function of T/η_s . The symbols in both (a) and (b) correspond to the HPC concentrations of $c = (\Delta)$ 4.98 and (\circ) 19.99 g/L.

tion of polymers because η_s at the sudden drop in Δn_{120} corresponded to T_p .

τ of polymer molecules is described by the following relation:

$$\tau \propto \frac{\eta_s R^3}{k_B T} \quad (2)$$

This relation is rewritten by eq.(1), which relates τ with $\dot{\epsilon}_c$:

$$\dot{\epsilon}_c \propto \frac{k_B T}{\eta_s R^3} \quad (3)$$

where η_s , k_B , and T represent the solvent viscosity, the Boltzmann constant, and the absolute temperature, respectively. R represents the molecular size, which is described by Einstein–Stoke's relation $R(c) = k_B T / 6\pi\eta_s D(c)$ for each concentration. In eq.(3), $\dot{\epsilon}_c$ is related not only to η_s but also to R . Figure 5(b) shows the T/η_s dependence of $\dot{\epsilon}_c$. In the one-phase region, $\dot{\epsilon}_c$ increased slightly with an increase in T/η_s , indicating a slight decrease in R with temperature. On the other hand, in

a larger T/η_s region where the sample was in a two-phase region, $\dot{\epsilon}_c$ decreased. This decrease in $\dot{\epsilon}_c$ was attributed to the rapid growth of apparent R , probably due to the association of the HPC chain. The sudden drop in Δn_{120} and $\dot{\epsilon}_c$ indicated that the elongational properties of the associated polymer chains were different from those of a single polymer.

Transition from flexible to rigid rod-like molecules

Figure 6 shows the temperature evolution of the birefringence pattern in HPC concentration of $c = 4.98$ g/L from $T = 28.9^\circ\text{C}$ (slightly below T_p) to $T = 32.4^\circ\text{C}$ (slightly below T_s). As the temperature increased higher than T_p , the coil-stretch transition-like pattern changed to a pattern typical to rigid rod-like polymers without $\dot{\epsilon}_c$. In addition to the rigid rod-like pattern, a second increase in Δn appeared in a higher $\dot{\epsilon}$ region. The second increase had the character of a coil-stretch transition with an apparent critical elongational strain rate ($\dot{\epsilon}_{c,\text{app}}$) and a localized birefringence pattern. In Figure 6, the arrows indicate $\dot{\epsilon}_{c,\text{app}}$. During the first increase in the two-stage evolution of Δn , a mixed birefringence pattern of a rod-like response and a weak localized line was observed. The weak localized pattern was intensified at $\dot{\epsilon}_{c,\text{app}}$. The second increase in Δn at $\dot{\epsilon}_{c,\text{app}}$ indicated the deformation of the cluster formed by the association of polymers. The cluster was considered to be not as rigid as rod-like molecules.

To relate the new feature in the Δn to the phase-separation process, it is useful for one to appreciate the temperature dependence of $\dot{\epsilon}_c$ and Δn_{120} in Figure 4. In the one-phase region, Δn_{120} decreased monotonously, but in the vicinity of T_p , a new tendency corresponding to the second increase in Δn appeared. The temperature at $\dot{\epsilon}_c(T) = 0$ in Figure 4 was related to the temperature at which the flexible polymer-like birefringent response completely changed to that of a rigid rod-like pattern. HPC is a semicrystalline polymer that consists of a crystallizable segment of cellulose and hydroxypropyl substituents. The transition in the birefringence pattern from a flexible-like pattern to a rigid rod-like pattern was attributed to the increase in the HPC chain rigidity by the molecular association through intermolecular and/or intramolecular hydrogen bondings. The rigid rod-like pattern was thought to be originated from the associated HPC polymer chains. As the association proceeded toward the liquid–crystalline droplet formation, with the temperature crossing the phase boundary, HPC chain cluster formation as the precursor for the liquid–crystalline phase was expected, and then Δn_{120} decreased.^{8,15,16,22} $\dot{\epsilon}_{c,\text{app}}$ was related to the extension of the aggregated cluster of the HPC chains. In the higher concentration region $c = 19.99$ g/L, although a typical rod-like pattern was not observed, the small shoulder in Δn_{120}

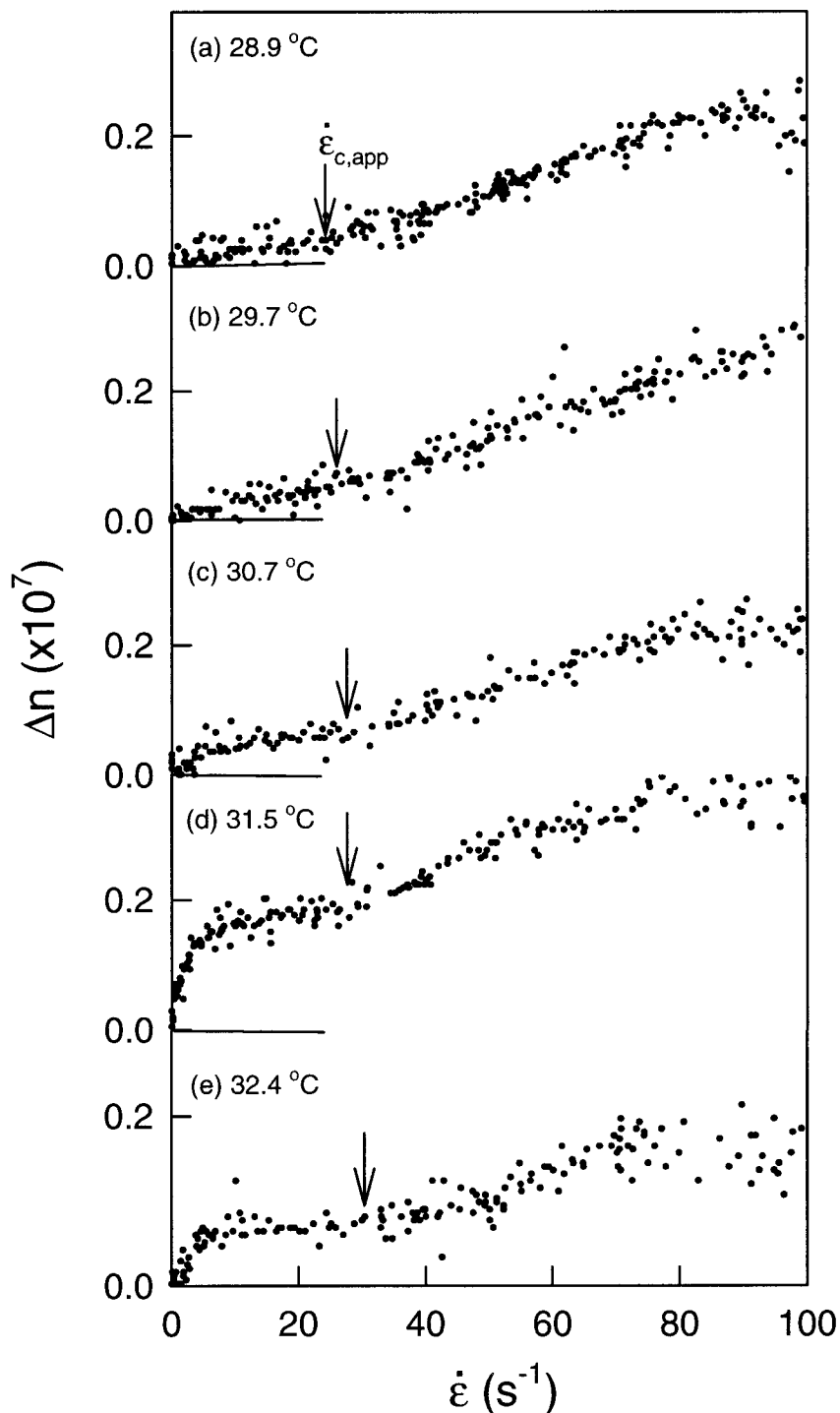


Figure 6 Δn as a function of strain rate at indicated temperatures slightly below and above T_p ; $T_p \approx 29.4^\circ\text{C}$ for HPC at a concentration of 4.98 g/L. $\dot{\epsilon}_{c,app}$ indicates the apparent critical elongational strain rate for the second increase in flow birefringence.

versus T plot near T_p indicates that the component of the rod-like response was probably added to the total birefringence intensity.

Figure 7 shows the rotational diffusion coefficient (D_r) for the HPC solution of 4.98 g/L, which was derived from Figure 6. D_r is determined from the birefringence intensity Δn by the following relation:^{10,13,23}

$$\Delta n = \Delta n_0 \frac{2\dot{\epsilon}}{15D_r} \tag{4}$$

where Δn_0 is the birefringence at a steady state in a rigid rod-like pattern. As the temperature increased, D_r gradually decreased. Because D_r is generally affected by a change in the aspect ratio of the molecule,

this decrease was attributed to the growing process of the HPC chain associates accompanied by the aspect ratio change. According to Doi and Edwards, the orientational order parameter (S) for a dilute solution of rigid rod-like polymers in an elongational flow field is described as²⁴

$$S = \frac{2}{3} \left[\frac{1}{4} - \frac{3}{2\xi} + \left(\frac{9}{16} - \frac{3}{4\xi} + \frac{9}{4\xi^2} \right)^{1/2} \right] \quad (5)$$

where ξ is the normalized strain rate with the rotational diffusion coefficient $\dot{\epsilon}/D_r$. S as a function of strain rate is shown in Figure 8, where we considered the associated HPC chain as rigid rod-like molecules. Curves from the bottom to top correspond to the order parameter of HPC molecules at the temperatures of 28.9, 29.7, 30.7, 31.5, and 32.4°C, respectively. In the calculation, the D_r presented in Figure 7 was used. In comparison with Figure 6, at 28.9°C, $\dot{\epsilon}_{c,app}$ was smaller than the strain rate at which the molecules could entirely orient in the elongational flow field. On the other hand, at 30.7, 31.5, and 32.4°C, the second increase in Δn_{120} appeared after molecules were entirely oriented along the elongational flow field. In the vicinity of the phase boundary, the rotational component of associated HPC chains seems to have only a small contribution.

Fortin et al. observed the onset of optical activity by measuring the circular dichroism in the vicinity of the phase-separation temperature at the concentration of 30 wt %, which was isotropic in the one-phase region at $T < T_p$. The optical activity was attributed to the appearance of cholesteric order in the polymer-rich phase.² The formation of the ordered liquid-crystalline phase, which is formed by anhydroglucose repeat units, is related to the rigidity of the cellulose backbone chain of HPC. When HPC undergoes phase sep-

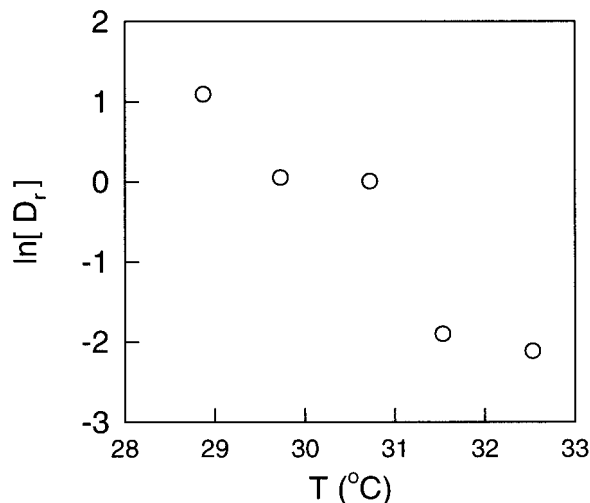


Figure 7 Semilogarithmic plot of D_r as a function of temperature for the HPC concentration of $c = 4.98$ g/L.

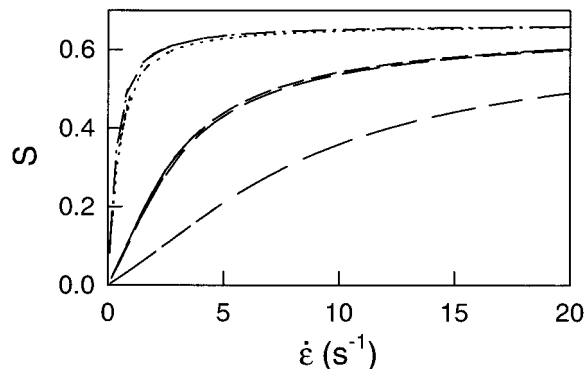


Figure 8 S as a function of $\dot{\epsilon}$ for HPC chains in an elongational flow field. For comparison with Figures 6 and 7(b), the abscissa is not the dimensionless strain rate ξ but $\dot{\epsilon}$. Curves correspond to 28.9, 29.7, 30.7, 31.5, and 32.4°C, respectively, from the bottom.

aration at a high temperature, the water structure along the hydrophobic hydroxypropyl substituents groups in HPC is expected to be broken, which causes the association of HPC molecules. This situation brings about the change in the structure of HPC molecules. Fischer et al. reported that the breaking of the water structure in the two-phase region caused the formation of a crystal solvate phase in the HPC-water system.⁴ In the transition of the birefringence pattern from flexible to rigid rod-like, we observed that the rigid rod-like response was related to the formation of an ordered liquid-crystalline-like structure of crystallizable segments.

CONCLUSIONS

The anomalous phase behavior by formation of a liquid-crystalline phase of HPC and the resultant elongational properties of the HPC chain in the phase-separation process were investigated by an elongational Δn method. In the one-phase region, HPC exhibited a response reminiscent of the coil-stretch transition of a flexible polymer chain. We observed $\dot{\epsilon}_c$ and the birefringence intensity Δn_{120} inside the phase boundary as a function of temperature at different concentrations. The temperature dependence of these parameters were found to have two-stage processes. The first stage was placed below T_p and was the stage where both $\dot{\epsilon}_c$ and Δn_{120} monotonously changed with temperature. The result was explained by the change in the relaxation time according to the change in η_s and HPC chain rigidity with temperature. In the vicinity of the phase boundary, the second stage appeared, which corresponded to the mixed birefringence pattern of a rigid rod-like pattern with that of a flexible coil. The rigid rod-like pattern indicated the HPC chain association, which was regarded as the precursor of the liquid-crystalline phase formation.

The authors are grateful to R. Somekawa for technical assistance in the refractive index measurement.

References

1. Guido, S. *Macromolecules* 1995, 28, 4530.
2. Fortin, S.; Charlet, G. *Macromolecules* 1989, 22, 2286.
3. Robitaille, L.; Turcotte, N.; Fortin, S.; Charlet, G. *Macromolecules* 1991, 24, 2413.
4. Fischer, H.; Murray, M.; Keller, A.; Odell, J. A. *J Mater Sci* 1995, 30, 4623.
5. L'arez-V, C.; Crescenzi, V.; Ciferri, A. *Macromolecules* 1995, 28, 5280.
6. Werbowyj, R. S.; Gray, D. G. *Macromolecules* 1980, 13, 69.
7. Flory, P. J. *Adv Polym Sci* 1984, 59, 1.
8. Shukla, P.; Muthukumar, M.; Langley, K. H. *J Appl Polym Sci* 1992, 44, 2115.
9. de Gennes, P. G. *J Chem Phys* 1974, 60, 5030.
10. Keller, A.; Odell, J. A. *Colloid Polym Sci* 1985, 263, 181.
11. Hayakawa, I.; Sasaki, N.; Hikichi, K. *Polymer* 1997, 39, 1393.
12. Hayakawa, I.; Hayashi, C.; Sasaki, N.; Hikichi, K. *J Appl Polym Sci* 1996, 61, 1731.
13. Sasaki, N.; Atkins, E. D. T.; Fulton, W. S. *J Appl Polym Sci* 1991, 42, 2975.
14. Wakabayashi, K.; Sasaki, N.; Hikichi, K. *J Appl Polym Sci* 2000, 76, 1351.
15. Chevillard, C.; Axelos, M. A. *Colloid Polym Sci* 1997, 275, 537.
16. Hirrien, M.; Chevillard, C.; Desbrieres, J.; Axelos, M. A.; Rinaudo, M. *Polymer* 1998, 39, 6251.
17. Tanaka, T.; Swislow, G.; Ohmine, I. *Phys Rev Lett* 1979, 42, 1556.
18. Taylor, G. I. *Proc R Soc Lond* 1934, 146, 501.
19. Torza, S. *J Polym Sci* 1975, 13, 43.
20. Sarkar, N. *J Appl Polym Sci* 1979, 24, 1073.
21. Segur, J. B.; Oberstar, H. E. *Ind Eng Chem* 1951, 43, 2117.
22. Morgenstern, B.; Kammer, H. W. *Polymer* 1999, 40, 1299.
23. Peterlin, A. *J Phys Chem* 1980, 84, 1650.
24. Doi, M.; Edwards, S. F. *The Theory of Polymer Dynamics*, Clarendon: Oxford, England, 1986; Chapter 8.